

Medium effects on the viscosities of a pion gas

Sukanya Mitra and Sourav Sarkar

Theoretical Physics Division, Variable Energy Cyclotron Centre,

1/AF Bidhannagar Kolkata - 700064, India

Abstract

The bulk and shear viscosities of a pion gas is obtained by solving the relativistic transport equation in the Chapman-Enskog approximation. In-medium effects are introduced in the $\pi\pi$ cross-section through one-loop self-energies in the propagator of the exchanged ρ . The effect of early chemical freeze-out in heavy ion collisions is implemented through a temperature dependent pion chemical potential. These are found to affect the temperature dependence of the bulk and shear viscosities significantly.

I. INTRODUCTION

The study of transport coefficients and non-equilibrium dynamics in general has assumed a great significance in recent times. The impetus in this direction has been provided by the recent results from the Relativistic Heavy Ion Collider (RHIC), in particular the elliptic flow which seems to be rather well described by nearly ideal hydrodynamics with a very low value of η/s , close to the quantum bound $1/4\pi$ [1], η and s being the coefficient of shear viscosity and entropy density respectively. This led to the description of quark gluon plasma as the most perfect fluid known [2].

Of the two viscosities used to parametrize the leading order corrections to the stress tensor the shear viscosity η is more commonly discussed, the magnitude of ζ the bulk viscosity usually being much smaller in comparison. The latter actually vanishes as in the case of systems with conformal invariance e.g. a gas of non-interacting highly relativistic particles. Breaking of conformal invariance of QCD due to quantum effects shows up through non-zero values of ζ which is related to the trace of the energy momentum tensor. An estimate of this can be obtained from the interaction measure determined from lattice calculations [3]. The behaviour of ζ and η as a function of temperature is particularly relevant in the context of non-ideal hydrodynamic simulations of heavy ion collisions. Whereas η/s as a function of T is expected to go through a minimum [2] at or near the critical value for crossover from the partonic phase, it is believed that ζ/s may be large [4] or even diverging close to this value. These have been studied in the linear sigma model in the large- N limit [5, 6] and for a massless pion gas in [7].

The viscosities of a pion gas have received some attention in recent times. In the diagrammatic approach, one uses the Kubo formula which relates the transport coefficients to retarded two-point functions [8, 9]. The shear viscosity of a pion gas in this approach was evaluated in [10, 11]. However, the kinetic theory approach being computationally more efficient [12], has been mostly used to obtain the viscous coefficients. The $\pi\pi$ cross-section is a crucial dynamical input in these calculations. Scattering amplitudes evaluated using chiral perturbation theory [13, 14] to lowest order have been used in [15, 16] and unitarization improved estimates of the amplitudes were used in [17] to evaluate the shear viscosity. Phenomenological scattering cross-section using experimental phase shifts have been used in [16, 18–20]. While in [21] the effect of number changing processes on the bulk viscosity

of a pion gas has been studied, in [22] unitarized chiral perturbation theory was used to demonstrate the breaking of conformal symmetry by the pion mass.

Our aim in this work is to construct the $\pi\pi$ cross-section in the medium and study its effect on the temperature dependence of the viscous coefficients. For this purpose we employ an effective Lagrangian approach which incorporates ρ and σ meson exchange in $\pi\pi$ scattering. A motivating factor is the role of the ρ pole in $\pi\pi$ scattering in preserving the quantum bound on η/s for a pion gas as demonstrated through use of the phenomenological [19, 23] and unitarized [17] cross-section in [24]. Medium effects are then introduced in the ρ propagator through one-loop self-energy diagrams. Now, the hadronic matter produced in highly relativistic heavy ion collisions is known to undergo early chemical freeze-out. Number changing (inelastic) processes having much larger relaxation times go out of equilibrium at this point and a temperature dependent chemical potential results for each species so as to conserve the number corresponding to the measured particle ratios. We thus evaluate the bulk and shear viscosity of a pion gas below the crossover temperature in heavy ion collisions considering only elastic $\pi\pi$ scattering in the medium with a temperature dependent pion chemical potential. In the process we extend our estimation of the shear viscosity at vanishing chemical potential [25] where a significant effect of the medium on the temperature dependence was observed.

In the next section, we briefly recapitulate the expressions for the viscosities obtained by solving the transport equation in the Chapman-Enskog approximation. In section III we describe the $\pi\pi$ cross-section in the medium. Numerical results are provided in section IV followed by summary and conclusions in section V.

II. THE BULK AND SHEAR VISCOSITY IN THE CHAPMAN-ENSKOG APPROXIMATION

The evolution of the phase space distribution of the pions is governed by the equation

$$p^\mu \partial_\mu f(x, p) = C[f] \quad (1)$$

where $C[f]$ is the collision integral. For binary elastic collisions $p + k \rightarrow p' + k'$ which we consider, this is given by [20]

$$C[f] = \int d\Gamma_k d\Gamma_{p'} d\Gamma_{k'} [f(x, p')f(x, k')\{1 + f(x, p)\}\{1 + f(x, k)\}$$

$$-f(x, p)f(x, k)\{1 + f(x, p')\}\{1 + f(x, k')\} W \quad (2)$$

where the interaction rate,

$$W = \frac{s}{2} \frac{d\sigma}{d\Omega} (2\pi)^6 \delta^4(p + k - p' - k')$$

and $d\Gamma_q = \frac{d^3q}{(2\pi)^3 q_0}$. The 1/2 factor comes from the indistinguishability of the initial state pions.

For small deviation from local equilibrium we write, in the first Chapman-Enskog approximation

$$f(x, p) = f^{(0)}(x, p) + \delta f(x, p), \quad \delta f(x, p) = f^{(0)}(x, p)[1 + f^{(0)}(x, p)]\phi(x, p) \quad (3)$$

where the equilibrium distribution function is given by

$$f^{(0)}(x, p) = \left[e^{\frac{p^\mu u_\mu(x) - \mu(x)}{T(x)}} - 1 \right]^{-1}, \quad (4)$$

with $T(x)$, $u_\mu(x)$ and $\mu(x)$ representing the local temperature, flow velocity and chemical potential respectively. Putting (3) in (1) the deviation function $\phi(x, p)$ is seen to satisfy

$$p^\mu \partial_\mu f^{(0)}(x, p) = -\mathcal{L}[\phi] \quad (5)$$

where the linearized collision term

$$\begin{aligned} \mathcal{L}[\phi] = & f^{(0)}(x, p) \int d\Gamma_k d\Gamma_{p'} d\Gamma_{k'} f^{(0)}(x, k) \{1 + f^{(0)}(x, p')\} \{1 + f^{(0)}(x, k')\} \\ & [\phi(x, p) + \phi(x, k) - \phi(x, p') - \phi(x, k')] W . \end{aligned} \quad (6)$$

Using the form of $f^{(0)}(x, p)$ as given in (4) on the left side of (5) and eliminating time derivatives with the help of equilibrium thermodynamic laws we arrive at

$$[Q\partial_\nu u^\nu - p_\mu \nabla^{\mu\nu} (p_\sigma u^\sigma + m_\pi h)(T^{-1}\partial_\nu T + Du_\nu) + \langle p_\mu p_\nu \rangle \langle \partial^\mu u^\nu \rangle] f^{(0)}(1 + f^{(0)}) = -T\mathcal{L}[\phi] \quad (7)$$

where $D = u^\mu \partial_\mu$, $\nabla_\mu = \Delta_{\mu\nu} \partial^\nu$, $\Delta_{\mu\nu} = g_{\mu\nu} - u_\mu u_\nu$ and $\langle \cdot \rangle$ indicates a space-like symmetric and traceless combination. In this equation

$$Q = -\frac{1}{3}m_\pi^2 + (p_\mu u^\mu)^2 \left\{ \frac{4}{3} - \gamma' \right\} + \{(\gamma'' - 1)m_\pi h - \gamma''' T\} p_\mu u^\mu \quad (8)$$

where

$$\gamma' = \frac{(S_2^0/S_2^{-1})^2 - (S_3^0/S_2^{-1})^2 + 4z^{-1}S_2^0 S_3^{-1}/(S_2^{-1})^2 + z^{-1}S_3^0/S_2^{-1}}{(S_2^0/S_2^{-1})^2 - (S_3^0/S_2^{-1})^2 + 3z^{-1}S_2^0 S_3^{-1}/(S_2^{-1})^2 + 2z^{-1}S_3^0/S_2^{-1} - z^{-2}} \quad (9)$$

$$\gamma'' = 1 + \frac{z^{-2}}{(S_2^0/S_2^{-1})^2 - (S_3^0/S_2^{-1})^2 + 3z^{-1}S_2^0S_3^{-1}/(S_2^{-1})^2 + 2z^{-1}S_3^0/S_2^{-1} - z^{-2}} \quad (10)$$

$$\gamma''' = \frac{S_2^0/S_2^{-1} + 5z^{-1}S_3^{-1}/S_2^{-1} - S_3^0S_3^{-1}/(S_2^{-1})^2}{(S_2^0/S_2^{-1})^2 - (S_3^0/S_2^{-1})^2 + 3z^{-1}S_2^0S_3^{-1}/(S_2^{-1})^2 + 2z^{-1}S_3^0/S_2^{-1} - z^{-2}} \quad (11)$$

with $z = m_\pi/T$, enthalpy $h = S_3^{-1}/S_2^{-1}$ and the function S_n^α is a polynomial given by $S_n^\alpha(z) = \sum_{k=1}^{\infty} e^{k\mu/T} k^\alpha K_n(kz)$, $K_n(x)$ denoting the modified Bessel function of order n . The left hand side of (5) is thus expressed in terms of thermodynamic forces with different tensorial ranks. In order to be a solution of this equation ϕ must also be a linear combination of the corresponding thermodynamic forces. It is typical to take ϕ as

$$\phi = A\partial_\nu u_\nu + B_\mu \nabla^{\mu\nu} (T^{-1}\partial_\nu T + Du_\nu) + C_{\mu\nu} \langle \partial^\mu u^\nu \rangle \quad (12)$$

which on substitution into (7) and comparing coefficients of the (independent) thermodynamic forces on both sides, yields the set of equations

$$\mathcal{L}[A] = -Qf^{(0)}(p)\{1 + f^{(0)}(p)\}/T \quad (13)$$

$$\mathcal{L}[C_{\mu\nu}] = -\langle p_\mu p_\nu \rangle f^{(0)}(p)\{1 + f^{(0)}(p)\}/T \quad (14)$$

ignoring the equation for B_μ which is related to thermal conductivity. These integral equations are to be solved to get the coefficients A and $C_{\mu\nu}$. It now remains to link these to the viscous coefficients ζ and η . This is achieved by means of the dissipative part of the energy-momentum tensor resulting from the use of the non-equilibrium distribution function (3) in

$$T^{\mu\nu} = \int d\Gamma_p p^\mu p^\nu f(p) = T^{\mu\nu(0)} + \Delta T^{\mu\nu} \quad (15)$$

where

$$\Delta T^{\mu\nu} = \int d\Gamma_p f^{(0)}(1 + f^{(0)})C_{\mu\nu} \langle p^\mu p^\nu \rangle \langle \partial^\mu u^\nu \rangle + \int d\Gamma_p f^{(0)}(1 + f^{(0)})QA\Delta^{\mu\nu} \partial_\sigma u^\sigma \quad (16)$$

Again, for a small deviation $\phi(x, p)$, close to equilibrium, so that only first order derivatives contribute, the dissipative tensor can be generally expressed in the form [26, 27]

$$\Delta T^{\mu\nu} = -2\eta \langle \partial^\mu u^\nu \rangle - \zeta \Delta^{\mu\nu} \partial_\sigma u^\sigma \quad (17)$$

Comparing, we obtain the expressions of shear and bulk viscosity,

$$\eta = -\frac{1}{10} \int d\Gamma_p C_{\mu\nu} \langle p^\mu p^\nu \rangle f^{(0)}(p)\{1 + f^{(0)}(p)\} \quad (18)$$

and

$$\zeta = - \int d\Gamma_p Q A f^{(0)}(p) \{1 + f^{(0)}(p)\} . \quad (19)$$

The coefficients A and $C_{\mu\nu}$ are perturbatively obtained from (13) and (14) by expanding in terms of orthogonal polynomials which reduces the integral equations to algebraic ones. After a tedious calculation using the Laguerre polynomial of 1/2 integral order, the first approximation to shear and bulk viscosity come out as

$$\eta = \frac{T}{10} \frac{\gamma_0^2}{c_{00}} \quad (20)$$

and

$$\zeta = T \frac{\alpha_2^2}{a_{22}} \quad (21)$$

where

$$\begin{aligned} \gamma_0 &= -10 \frac{S_3^{-2}(z)}{S_2^{-1}(z)} , \\ c_{00} &= 16I_1(z) + 16I_2(z) + \frac{16}{3}I_3(z) . \end{aligned} \quad (22)$$

and

$$\begin{aligned} \alpha_2 &= \frac{z^3}{2} \left[\frac{1}{3} \left(\frac{S_3^0}{S_2^{-1}} - z^{-1} \right) + \left(\frac{S_2^0}{S_2^{-1}} + \frac{3}{z} \frac{S_3^{-1}}{S_2^{-1}} \right) \left\{ (1 - \gamma'') \frac{S_3^{-1}}{S_2^{-1}} + \gamma''' z^{-1} \right\} \right. \\ &\quad \left. - \left(\frac{4}{3} - \gamma' \right) \left\{ \frac{S_3^0}{S_2^{-1}} + 15z^{-2} \frac{S_3^{-2}}{S_2^{-1}} + 2z^{-1} \right\} \right] , \\ a_{22} &= \frac{3}{8} z^2 I_3(z) . \end{aligned} \quad (23)$$

The integrals $I_\alpha(z)$ are given by

$$\begin{aligned} I_\alpha(z) &= \frac{z^4}{[S_2^{-1}(z)]^2} e^{(-2\mu/T)} \int_0^\infty d\psi \cosh^3 \psi \sinh^7 \psi \int_0^\pi d\Theta \sin \Theta \frac{1}{2} \frac{d\sigma}{d\Omega}(\psi, \Theta) \int_0^{2\pi} d\phi \\ &\quad \int_0^\infty d\chi \sinh^{2\alpha} \chi \int_0^\pi d\theta \sin \theta \frac{e^{2z \cosh \psi \cosh \chi}}{(e^E - 1)(e^F - 1)(e^G - 1)(e^H - 1)} M_\alpha(\theta, \Theta) \end{aligned} \quad (24)$$

where μ is the chemical potential of pions. The exponents in the Bose functions are given by

$$\begin{aligned} E &= z(\cosh \psi \cosh \chi - \sinh \psi \sinh \chi \cos \theta) \\ F &= z(\cosh \psi \cosh \chi - \sinh \psi \sinh \chi \cos \theta') \\ G &= E + 2z \sinh \psi \sinh \chi \cos \theta \\ H &= F + 2z \sinh \psi \sinh \chi \cos \theta' , \end{aligned} \quad (25)$$

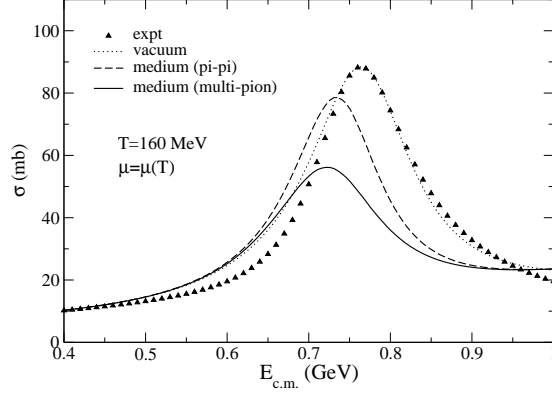


FIG. 1: The $\pi\pi$ cross-section as a function of centre of mass energy. The dotted line indicates the cross-section obtained using eq. (30) which agrees well with the experimental values (eq. (27)) shown by filled triangles. The dashed and solid lines depict the in-medium cross-section for $\pi\pi$ and πh loops respectively in the ρ self-energy evaluated at $T=160$ MeV with temperature dependent pion chemical potential.

and the functions M are defined as

$$\begin{aligned}
 M_1(\theta, \Theta) &= 1 - \cos^2 \Theta , \\
 M_2(\theta, \Theta) &= \cos^2 \theta + \cos^2 \theta' - 2 \cos \theta \cos \theta' \cos \Theta , \\
 M_3(\theta, \Theta) &= [\cos^2 \theta - \cos^2 \theta']^2
 \end{aligned} \tag{26}$$

The relative angle θ' is defined by, $\cos \theta' = \cos \theta \cos \Theta - \sin \theta \sin \Theta \cos \phi$.

Note that the differential cross-section which appears in the denominator is the dynamical input in the expressions for η and ζ . It is this quantity we turn to in the next section.

III. THE $\pi\pi$ CROSS-SECTION WITH MEDIUM EFFECTS

The strong interaction dynamics of the pions enters the collision integrals through the cross-section. In Fig. 1 we show the $\pi\pi$ cross-section as a function of the centre of mass energy of scattering. The different curves are explained below. The filled triangles referred to as experiment is a widely used resonance saturation parametrization [19, 23] of isoscalar and isovector phase shifts obtained from various empirical data involving the $\pi\pi$ system. The isospin averaged differential cross-section is given by

$$\frac{d\sigma(s)}{d\Omega} = \frac{4}{q_{cm}^2} \left[\frac{1}{9} \sin^2 \delta_0^0 + \frac{5}{9} \sin^2 \delta_0^2 + \frac{1}{3} \cdot 9 \sin^2 \delta_1^1 \cos^2 \theta \right] \tag{27}$$

where

$$\begin{aligned}
\delta_0^0 &= \frac{\pi}{2} + \arctan\left(\frac{E - m_\sigma}{\Gamma_\sigma/2}\right) \\
\delta_1^1 &= \frac{\pi}{2} + \arctan\left(\frac{E - m_\rho}{\Gamma_\rho/2}\right) \\
\delta_0^2 &= -0.12p/m_\pi .
\end{aligned} \tag{28}$$

The widths are given by $\Gamma_\sigma = 2.06p$ and $\Gamma_\rho = 0.095p \left(\frac{p/m_\pi}{1+(p/m_\rho)^2}\right)^2$ with $m_\sigma = 5.8m_\pi$ and $m_\rho = 5.53m_\pi$.

To get a handle on the dynamics we now evaluate the $\pi\pi$ cross-section involving ρ and σ meson exchange processes using the interaction Lagrangian

$$\mathcal{L} = g_\rho \vec{\rho}^\mu \cdot \vec{\pi} \times \partial_\mu \vec{\pi} + \frac{1}{2} g_\sigma m_\sigma \vec{\pi} \cdot \vec{\pi} \sigma \tag{29}$$

where $g_\rho = 6.05$ and $g_\sigma = 2.5$. In the matrix elements corresponding to s -channel ρ and σ exchange diagrams which appear for total isospin $I = 1$ and 0 respectively, we introduce a decay width in the corresponding propagator. We get [25],

$$\begin{aligned}
\mathcal{M}_{I=0} &= g_\sigma^2 m_\sigma^2 \left[\frac{3}{s - m_\sigma^2 + im_\sigma \Gamma_\sigma} + \frac{1}{t - m_\sigma^2} + \frac{1}{u - m_\sigma^2} \right] + 2g_\rho^2 \left[\frac{s - u}{t - m_\rho^2} + \frac{s - t}{u - m_\rho^2} \right] \\
\mathcal{M}_{I=1} &= g_\sigma^2 m_\sigma^2 \left[\frac{1}{t - m_\sigma^2} - \frac{1}{u - m_\sigma^2} \right] + g_\rho^2 \left[\frac{2(t - u)}{s - m_\rho^2 + im_\rho \Gamma_\rho(s)} + \frac{t - s}{u - m_\rho^2} - \frac{u - s}{t - m_\rho^2} \right] \\
\mathcal{M}_{I=2} &= g_\sigma^2 m_\sigma^2 \left[\frac{1}{t - m_\sigma^2} + \frac{1}{u - m_\sigma^2} \right] + g_\rho^2 \left[\frac{u - s}{t - m_\rho^2} + \frac{t - s}{u - m_\rho^2} \right].
\end{aligned} \tag{30}$$

The differential cross-section is then obtained from $\frac{d\sigma}{d\Omega} = |\overline{\mathcal{M}}|^2/64\pi^2 s$ where the isospin averaged amplitude is given by $|\overline{\mathcal{M}}|^2 = \frac{1}{9} \sum (2I + 1) |\overline{\mathcal{M}}_I|^2$.

The integrated cross-section, after ignoring the $I = 2$ contribution is shown by the dotted line (indicated by 'vacuum') in Fig. 1 and is seen to agree reasonably well with the experimental cross-section up to a centre of mass energy of about 1 GeV beyond which the theoretical estimate gives higher values. We hence use the experimental cross-section beyond this energy.

After this normalisation to data, we now turn to the in-medium cross-section by introducing the effective propagator for the ρ in the above expressions for the matrix elements. This is obtained in terms of the self-energy by solving the Dyson equation and is given by

$$D_{\mu\nu} = D_{\mu\nu}^{(0)} + D_{\mu\sigma}^{(0)} \Pi^{\sigma\lambda} D_{\lambda\nu} \tag{31}$$

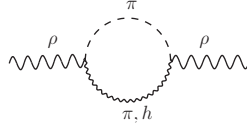


FIG. 2: $\pi\pi$ and πh self-energy diagrams where h stands for ω, h_1, a_1 mesons.

where $D_{\mu\nu}^{(0)}$ is the vacuum propagator for the ρ meson and $\Pi^{\sigma\lambda}$ is the self energy function obtained from one-loop diagrams shown in Fig. 2. The standard procedure [28] to solve this equation in the medium is to decompose the self-energy into transverse and longitudinal components. For the case at hand the difference between these components is found to be small and is hence ignored. We work with the polarization averaged self-energy function defined as

$$\Pi = \frac{1}{3}(2\Pi^T + q^2\Pi^L) \quad (32)$$

where

$$\Pi^T = -\frac{1}{2}(\Pi_\mu^\mu + \frac{q^2}{\vec{q}^2}\Pi_{00}), \quad \Pi^L = \frac{1}{\vec{q}^2}\Pi_{00}, \quad \Pi_{00} \equiv u^\mu u^\nu \Pi_{\mu\nu} . \quad (33)$$

The in-medium propagator is then written as

$$D_{\mu\nu}(q_0, \vec{q}) = \frac{-g_{\mu\nu} + q_\mu q_\nu / q^2}{q^2 - m_\rho^2 - \text{Re}\Pi(q_0, \vec{q}) + i\text{Im}\Pi(q_0, \vec{q})} . \quad (34)$$

The scattering, decay and regeneration processes which cause a gain or loss of ρ mesons in the medium are responsible for the imaginary part of its self-energy. The real part on the other hand modifies the position of the pole of the spectral function.

In the real-time formulation of thermal field theory the self-energy assumes a 2×2 matrix structure of which the 11-component is given by

$$\Pi_{\mu\nu}^{11}(q) = i \int \frac{d^4k}{(2\pi)^4} N_{\mu\nu}(q, k) D_\pi^{11}(k) D_h^{11}(q - k) \quad (35)$$

where D^{11} is the 11-component of the scalar propagator given by $D^{11}(k) = \Delta(k) + 2\pi i f^{(0)}(k) \delta(k^2 - m^2)$. It turns out that the self-energy function mentioned above can be obtained in terms of the 11-component through the relations [28, 29]

$$\begin{aligned} \text{Re}\Pi_{\mu\nu} &= \text{Re}\Pi_{\mu\nu}^{11} \\ \text{Im}\Pi_{\mu\nu} &= \epsilon(q_0) \tanh(\beta q_0/2) \text{Im}\Pi_{\mu\nu}^{11} . \end{aligned} \quad (36)$$

Tensor structures associated with the two vertices and the vector propagator are included in $N_{\mu\nu}$ and are available in [30] where the interactions were taken from chiral perturbation theory. It is easy to perform the integral over k_0 using suitable contours to obtain

$$\begin{aligned} \Pi^{\mu\nu}(q_0, \vec{q}) = & \int \frac{d^3k}{(2\pi)^3} \frac{1}{4\omega_\pi\omega_h} \left[\frac{(1 + f^{(0)}(\omega_\pi))N_1^{\mu\nu} + f^{(0)}(\omega_h)N_3^{\mu\nu}}{q_0 - \omega_\pi - \omega_h + i\eta\epsilon(q_0)} + \frac{-f^{(0)}(\omega_\pi)N_1^{\mu\nu} + f^{(0)}(\omega_h)N_4^{\mu\nu}}{q_0 - \omega_\pi + \omega_h + i\eta\epsilon(q_0)} \right. \\ & \left. + \frac{f^{(0)}(\omega_\pi)N_2^{\mu\nu} - f^{(0)}(\omega_h)N_3^{\mu\nu}}{q_0 + \omega_\pi - \omega_h + i\eta\epsilon(q_0)} + \frac{-f^{(0)}(\omega_\pi)N_2^{\mu\nu} - (1 + f^{(0)}(\omega_h))N_4^{\mu\nu}}{q_0 + \omega_\pi + \omega_h + i\eta\epsilon(q_0)} \right] \quad (37) \end{aligned}$$

where $f^{(0)}(\omega) = \frac{1}{e^{(\omega-\mu)/T}-1}$ is the Bose distribution function with arguments $\omega_\pi = \sqrt{\vec{k}^2 + m_\pi^2}$ and $\omega_h = \sqrt{(\vec{q} - \vec{k})^2 + m_h^2}$. Note that this expression is a generalized form for the in-medium self-energy obtained by Weldon [31]. The subscript $i(= 1, ..4)$ on $N^{\mu\nu}$ in (37) correspond to its values for $k_0 = \omega_\pi, -\omega_\pi, q_0 - \omega_h, q_0 + \omega_h$ respectively. It is easy to read off the real and imaginary parts from (37). The angular integration can be carried out using the δ -functions in each of the four terms in the imaginary part which define the kinematically allowed regions in q_0 and \vec{q} where scattering, decay and regeneration processes occur in the medium leading to the loss or gain of ρ mesons [30]. The vector mesons ω, h_1 and a_1 which appear in the loop have negative G -parity and have substantial 3π and $\rho\pi$ decay widths [32]. The (polarization averaged) self-energies containing these unstable particles in the loop graphs have thus been folded with their spectral functions,

$$\Pi(q, m_h) = \frac{1}{N_h} \int_{(m_h-2\Gamma_h)^2}^{(m_h+2\Gamma_h)^2} dM^2 \frac{1}{\pi} \text{Im} \left[\frac{1}{M^2 - m_h^2 + iM\Gamma_h(M)} \right] \Pi(q, M) \quad (38)$$

with $N_h = \int_{(m_h-2\Gamma_h)^2}^{(m_h+2\Gamma_h)^2} dM^2 \frac{1}{\pi} \text{Im} \left[\frac{1}{M^2 - m_h^2 + iM\Gamma_h(M)} \right]$. The contributions from the loops with heavy mesons (the πh loops) may then be considered as a multi-pion contribution to the ρ self-energy.

The in-medium cross-section is now obtained by using the full ρ -propagator (34) in place of the usual vacuum propagator $D_{\mu\nu}^{(0)}$ in the scattering amplitudes. The long dashed line in Fig. 1 shows a suppression of the peak when only the $\pi\pi$ loop is considered. This effect is magnified when both $\pi\pi$ and πh loops (solid line indicated by multi-pion) are taken into account and is also accompanied by a small shift in the peak position. Extension to the case of finite baryon density can be done using the spectral function computed in [33] where an extensive list of baryon (and anti-baryon) loops are considered along with the mesons. A similar modification of the $\pi\pi$ cross-section for a hot and dense system was seen also in [34].

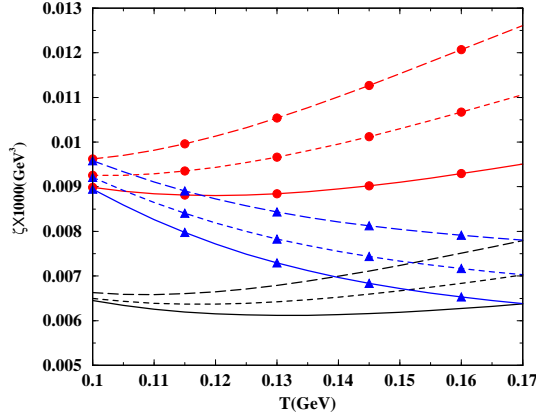


FIG. 3: (Color online) The bulk viscosity in various scenarios as a function of T . The various plots are explained in the text.

We end this section with a discussion of the pion chemical potential. As mentioned in the introduction, in heavy ion collisions pions get out of chemical equilibrium early at $T \sim 170$ MeV and a corresponding chemical potential starts building up with decrease in temperature. The kinetics of the gas is then dominated by elastic collisions including resonance formation such as $\pi\pi \leftrightarrow \rho$ etc. At still lower temperature, $T \sim 100$ MeV elastic collisions become rarer and the momentum distribution gets frozen resulting in kinetic freeze-out. This scenario is quite compatible with the treatment of medium modification of the $\pi\pi$ cross-section being employed in this work where the $\pi\pi$ interaction is mediated by ρ and σ exchange and the subsequent propagation of the ρ is modified by two-pion and effective multi-pion fluctuations. We take the temperature dependent pion chemical potential from Ref. [35] which implements the formalism described in [36]. The chemical potentials of the heavy mesons are then determined from elementary processes. The ω chemical potential e.g. is given by $\mu_\omega = 3 \times 0.88\mu$ where μ is the pion chemical potential, as a consequence of the processes $\omega \leftrightarrow \pi\pi\pi$ occurring in the medium. The branching ratios are taken from [32].

IV. RESULTS

We begin with the results for bulk viscosity ζ as a function of temperature T . In Fig. 3 the three sets of curves correspond to different values of the pion chemical potential. The uppermost set of curves (with circles) show the bulk viscosity calculated with a pion chemical potential $\mu \sim 85$ MeV. The corresponding curves in the lowermost set are evaluated with

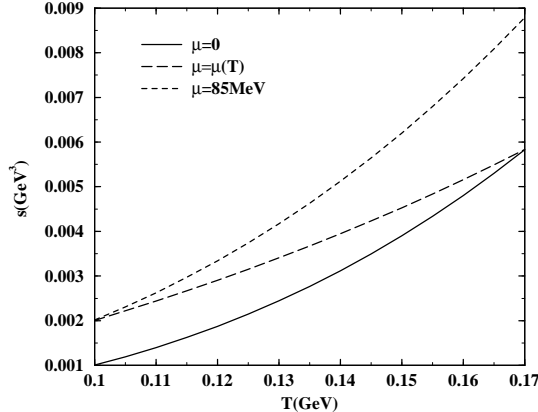


FIG. 4: The entropy density as a function of T for different values of the pion chemical potential.

$\mu = 0$. These values are representative of the kinetic and chemical freeze-out in heavy ion collisions respectively. The solid line in the lowermost set represents the case where the vacuum cross-section given by eq. (30) is used and agrees with the estimate in [20]. The set of curves with triangles depicts the situation when μ is a (decreasing) function of temperature as shown in [35]. This resembles the situation encountered in the later stages of heavy ion collisions and interpolates between the results with the constant values of the pion chemical potential discussed before. The three curves in each set show the effect of medium on the $\pi\pi$ cross-section. The short-dashed lines in each of the sets depict medium effects for pion loops in the ρ propagator and the long dashed lines correspond to the situation when the heavy mesons are included i.e. for both $\pi\pi$ and πh loops where $h = \omega, h_1, a_1$. The separation between the curves in each set displays a significant effect brought about by the medium dependence of the cross-section. A large dependence on the pion chemical potential is also inferred since the three sets of curves appear nicely separated.

Viscosities for relativistic fluids are generally expressed in terms of a dimensionless ratio obtained by dividing with the entropy density. The latter is obtained from the thermodynamic relation

$$Ts = \epsilon + P - n\mu \quad (39)$$

where

$$n = g_\pi \int d\Gamma_p E_p f^{(0)}(p),$$

$$\epsilon = g_\pi \int d\Gamma_p E_p^2 f^{(0)}(p),$$

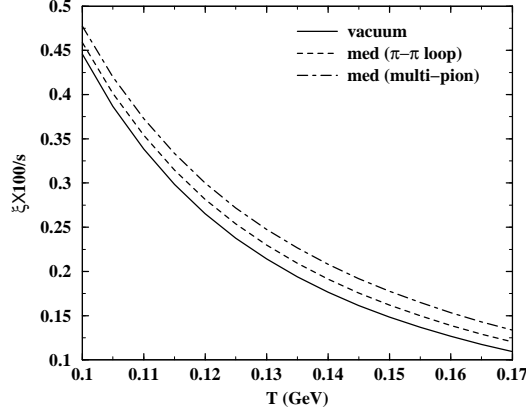


FIG. 5: ζ/s as a function of T for different $\pi\pi$ cross-section.

$$P = g_\pi \int d\Gamma_p \frac{\vec{p}^2}{3} f^{(0)}(p) , \quad (40)$$

and can be compactly expressed as

$$s = \frac{g_\pi m_\pi^2}{2\pi^2} (m_\pi S_3^{-1}(z) - \mu S_2^{-1}(z)) . \quad (41)$$

Here $g_\pi = 3$, $z = m_\pi/T$ and the functions $S_n^\alpha(z)$ are defined above. In Fig. 4 the entropy density of a pion gas as a function of temperature is shown for three values of the pion chemical potential as discussed in the context of Fig. 3.

In Fig. 5 we show ζ/s as a function of T using the temperature dependent pion chemical potential. The medium dependence is clearly observed when we compare the results obtained with the vacuum cross-section with the ones where the ρ propagation is modified due to the $\pi\pi$ and πh (multi-pion) loops. The decreasing trend with increasing temperature was observed also in [21] and [37].

We now turn to the shear viscosity. Here we extend the work in Ref. [25] to include the effect of the pion chemical potential. Shown in Fig. 6 is the shear viscosity as a function of T where the results with $\pi\pi$ and πh loops are contrasted with the case where the vacuum cross-section is used. The result for the experimental cross-section agrees with [17] and [20] for $\mu = 0$. A noticeable medium effect is observed as indicated by the short and long-dashed lines.

Finally, in Fig. 7 we show results for η/s . For $\mu = 0$ the upper set of curves with filled circles show the usual decreasing trend as seen, for example in [38]. This trend is reversed when $\mu(T)$ is used and η/s increases with T in contrast to ζ/s which decreases. The values

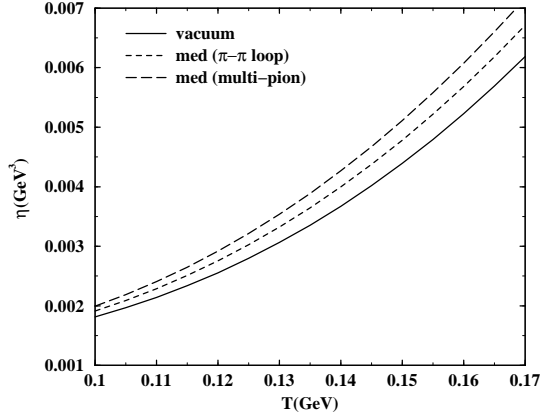


FIG. 6: η as a function of T for different values of the $\pi\pi$ cross-section.

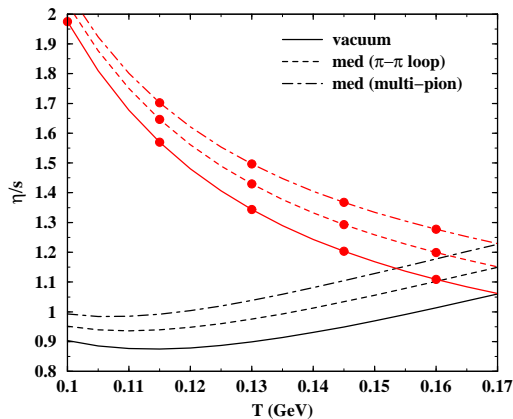


FIG. 7: (Color online) η/s as a function of T

in all cases remain well above the quantum bound.

V. SUMMARY AND OUTLOOK

In this work we have evaluated the viscosities of a pion gas by solving the Uehling-Uhlenbeck transport equation in the Chapman-Enskog approximation to leading order with an aim to study the effect of a medium dependent cross-section. The $\pi\pi$ cross-section which goes as an input to these calculations is evaluated from σ and ρ exchange processes. Spectral modifications of the ρ propagator implemented through $\pi\pi$ and πh self-energy diagrams shows a significant effect on the cross-section and consequently on the temperature dependence of transport coefficients. The effect of early chemical freeze-out in heavy ion collisions is implemented through a temperature dependent pion chemical potential which

also enhances the medium effect. Results for ζ/s and η/s also show a significant medium dependence in this scenario.

The viscous coefficients and their temperature dependence could affect the quantitative estimates of signals of heavy ion collisions particularly where hydrodynamic simulations are involved. For example, it has been argued in [39] that corrections to the freeze-out distribution due to bulk viscosity can be significant. As a result the hydrodynamic description of the p_T spectra and elliptic flow of hadrons could be improved by including a realistic temperature dependence of the viscous coefficients. Studies in this direction are in progress.

-
- [1] P. Kovtun, D. T. Son and A. O. Starinets, Phys. Rev. Lett. **94**, 111601 (2005).
 - [2] L. P. Csernai, J. I. Kapusta and L. D. McLerran, Phys. Rev. Lett. **97**, 152303 (2006).
 - [3] M. Cheng *et al.*, Phys. Rev. D **81** (2010) 054504
 - [4] D. Kharzeev and K. Tuchin, JHEP **0809** (2008) 093
 - [5] A. Dobado, F. J. Llanes-Estrada and J. M. Torres-Rincon, Phys. Rev. D **80** (2009) 114015
 - [6] A. Dobado and J. M. Torres-Rincon, Phys. Rev. D **86** (2012) 074021
 - [7] J. -W. Chen and J. Wang, Phys. Rev. C **79** (2009) 044913
 - [8] D. N. Zubarev, *Non-equilibrium Statistical Thermodynamics* (Consultants Bureau, NN, 1974).
 - [9] A. Hosoya, M. a. Sakagami and M. Takao, Annals Phys. **154** (1984) 229.
 - [10] R. Lang, N. Kaiser and W. Weise, Eur. Phys. J. A **48** (2012) 109
 - [11] S. Mallik and S. Sarkar, arXiv:1211.2588 [nucl-th].
 - [12] S. Jeon and L. G. Yaffe, Phys. Rev. D **53**, 5799 (1996).
 - [13] S. Weinberg, Physica A **96** (1979) 327.
 - [14] J. Gasser and H. Leutwyler, Annals Phys. **158**, 142 (1984).
 - [15] A. Dobado and S. N. Santalla, Phys. Rev. D **65**, 096011 (2002).
 - [16] J. W. Chen, Y. H. Li, Y. F. Liu and E. Nakano, Phys. Rev. D **76**, 114011 (2007)
 - [17] A. Dobado and F. J. Llanes-Estrada, Phys. Rev. D **69**, 116004 (2004).
 - [18] K. Itakura, O. Morimatsu and H. Otomo, Phys. Rev. D **77**, 014014 (2008).
 - [19] M. Prakash, M. Prakash, R. Venugopalan and G. Welke, Phys. Rept. **227** (1993) 321.
 - [20] D. Davesne, Phys. Rev. C **53**, 3069 (1996).
 - [21] E. Lu and G. D. Moore, Phys. Rev. C **83** (2011) 044901

- [22] D. Fernandez-Fraile and A. Gomez Nicola, Phys. Rev. Lett. **102** (2009) 121601
- [23] G. Bertsch, M. Gong, L. D. McLerran, P. V. Ruuskanen and E. Sarkkinen, Phys. Rev. D **37** (1988) 1202.
- [24] A. Dobado and F. J. Llanes-Estrada, Eur. Phys. J. C **49** (2007) 1011
- [25] S. Mitra, S. Ghosh and S. Sarkar, Phys. Rev. C **85** (2012) 064917
- [26] P. Chakraborty and J. I. Kapusta, Phys. Rev. C **83** (2011) 014906.
- [27] W. A. Van Leeuwen, P. H. Polak and S. R. De Groot, Physica **66**, 455 (1973).
- [28] M. Le Bellac, *Thermal Field Theory* (Cambridge University Press, Cambridge, 1996).
- [29] S. Mallik and S. Sarkar, Eur. Phys. J. C **61**, 489 (2009).
- [30] S. Ghosh, S. Sarkar and S. Mallik, Eur. Phys. J. C **70**, 251 (2010).
- [31] H. A. Weldon, Phys. Rev. D **28** (1983) 2007.
- [32] K. Nakamura *et al.* [Particle Data Group], J. Phys. G **37** (2010) 075021.
- [33] S. Ghosh and S. Sarkar, Nucl. Phys. A **870-871**, 94 (2011)
- [34] H. W. Barz, H. Schulz, G. Bertsch and P. Danielewicz, Phys. Lett. B **275** (1992) 19.
- [35] T. Hirano and K. Tsuda, Phys. Rev. C **66** (2002) 054905
- [36] H. Bebie, P. Gerber, J. L. Goity and H. Leutwyler, Nucl. Phys. B **378** (1992) 95.
- [37] A. Dobado, F. J. Llanes-Estrada and J. M. Torres-Rincon, Phys. Lett. B **702** (2011) 43
- [38] E. Nakano, hep-ph/0612255.
- [39] K. Dusling and T. Schafer, Phys. Rev. C **85** (2012) 044909